

**UNCLASSIFIED**

**Defense Technical Information Center  
Compilation Part Notice**

**ADP012596**

**TITLE:** Raman and Photoluminescence Mapping of Lattice Matched InGaP/GaAs Heterostructures

**DISTRIBUTION:** Approved for public release, distribution unlimited

This paper is part of the following report:

**TITLE:** Progress in Semiconductor Materials for Optoelectronic Applications Symposium held in Boston, Massachusetts on November 26-29, 2001.

To order the complete compilation report, use: ADA405047

The component part is provided here to allow users access to individually authored sections of proceedings, annals, symposia, etc. However, the component should be considered within the context of the overall compilation report and not as a stand-alone technical report.

The following component part numbers comprise the compilation report:

ADP012585 thru ADP012685

**UNCLASSIFIED**

## RAMAN AND PHOTOLUMINESCENCE MAPPING OF LATTICE MATCHED InGaP/GaAs HETEROSTRUCTURES

G. Attolini, P. Fallini, F. Germini, C. Pelosi

MASPEC-CNR Institute, Parco Area Delle Scienze, 37/A Fontanini, 43010 Parma, Italy

O. Martínez, L.F. Sanz, M.A. González, J. Jiménez

Física de la Materia Condensada, ETSII, 47011 Valladolid, Spain

### ABSTRACT

The influence of the substrate on composition and CuPt-type spontaneous order of MOVPE lattice matched InGaP/GaAs layers was studied. The study was carried out by microRaman and microphotoluminescence. The order was determined by the band gap, while the Raman parameters were also contributed by the surface topography that was also related to the type of substrate. The spontaneous order increases with Si- doping of the substrates. Doping the layers with Zn randomises the alloy.

### INTRODUCTION

InGaP layers lattice matched to GaAs substrates have potential applications for electronic devices, e.g. high efficiency tandem solar cells, single heterojunction bipolar transistors, tunable laser diodes, etc. It has some advantages in relation to AlGaAs ternary alloys, which are the base of many devices. Lattice matched InGaP presents a direct band gap of 1.9 eV, which is approximately equal to the maximum direct band gap that can be obtained with AlGaAs (Ga molar fraction of 0.4) [1]. InGaP is insensitive to oxygen and humidity inside the reactor, which is a well known cause of Al instability in AlGaAs [2].

InGaP is affected by other problems, in particular the composition control and the existence of an spontaneous ordered phase.  $\text{In}_{1-x}\text{Ga}_x\text{P}$  matches the GaAs lattice for  $x=0.516$  at room temperature; however due to the large lattice and thermal mismatches between InP, GaP and GaAs the composition is critical to avoid residual strain in the layers [3]. The second problem of interest regards the spontaneous order. InGaP can appear under a CuPt-type ordered phase [4, 5]. In the ordered phase the cations are not randomly distributed, but segregate spontaneously into alternate (111) planes giving a CuPt-type structure in the cation sublattice. This phase critically influences the optical and electrical properties of InGaP/GaAs layers. The most important is the shrinking of the band gap, which can be reduced by 100 meV for lattice matched composition [5, 6]. Also, the minority carrier lifetime and mobility are sensitive to cation order [6]. The spontaneous order is related to the growth method and the specific growth conditions, such as the substrate temperature and the V/III ratio. The nature of the susbstrate is shown here to influence the properties of the layers.

We present herein a detailed study of the properties of InGaP layers grown by LP-MOVPE (Low pressure metal organic vapor phase epitaxy) on different substrates aiming to understand the influence of the substrate on the spontaneous order. The analysis is carried out by High Resolution X-Ray diffraction (HRXRD), Atomic Force Microscopy (AFM), micro-Raman ( $\mu$ -R) and micro-Photoluminescence ( $\mu$ -PL).

## EXPERIMENTAL AND SAMPLES

Layers were grown at reduced pressure (60 mBar) by MOVPE in a horizontal reactor. The precursors were trimethylgallium (TMG), trimethylindium (TMI) and Phosphine ( $\text{PH}_3$ ) and Arsine ( $\text{AsH}_3$ ) as main reagents; arsine was diluted in hydrogen (5%). The layers of InGaP were deposited on (100) GaAs substrates cut 2° off towards the [110] axis. The growth conditions were the same for all runs, namely substrate temperature of 600°C and V/III ratio of 159.60 (rel.u.). The substrates were either semiinsulating (SI) or n-type (Si-doped), the doping level of the substrate was monitored by Raman spectroscopy, using the LO phonon-plasmon coupled (LOPC) modes; samples B, D, I and J were grown on semiinsulating substrates, samples F and H were grown on Si-doped substrates ( $[\text{Si}] > 3 \times 10^{18} \text{ cm}^{-3}$ ). The InGaP layers were either undoped (B, D, F and H) Si (J) or Zn (I) doped.

The AFM images show that the surface morphology of the InGaP layers was determined by the type of substrate, figure 1. In particular, layers grown on n-type substrates present flat surfaces suggesting layer by layer growth. Instead of this, layers grown on SI substrates exhibited a rough surface, looking like an array of parallel ridges about 0.2 μm wide, which exposes (100), (101) and (111) planes.

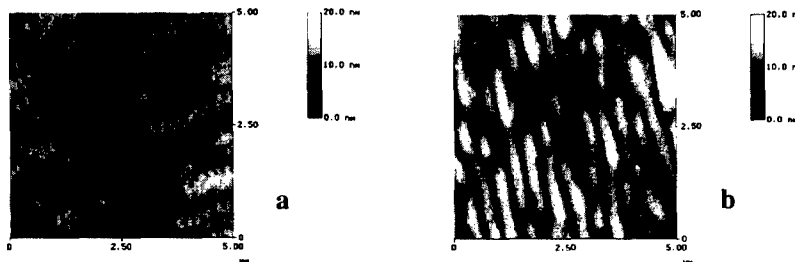


**Figure 1.** AFM images of samples grown on n-type substrates (Si-doped) (a), and semiinsulating substrates (b)

The layers were investigated by HRXRD. Two ( $R=0,\pi$ ) symmetric 004 reflections,  $R$  being the azimuthal angle, have been measured from each sample to eliminate the effect of a possible miscut angle. All the diffraction profiles were recorded in the  $\omega 2\theta$  scan mode. To estimate the perpendicular mismatch ( $\Delta d/d$ )<sup>4</sup> we used the first order formula  $(\Delta d/d)^4 = -\Delta\omega \cotg\theta_B$ , where  $\theta_B$  is the Bragg angle of the substrate and  $\Delta\omega$  the peak separation in arcsec.

$\mu$ -R measurements were carried out with a DILOR XY Raman spectrometer attached to a metallographic microscope. The 514.9 nm line of an  $\text{Ar}^+$  laser was focused onto the sample by the large numerical aperture (NA=0.95) of the microscope objective, which also collected the scattered light, conforming a nearly backscattering geometry. In our usual experimental conditions the laser beam diameter at the focal plane was slightly sub-micrometric.

Room temperature luminescence spectra were obtained in the same DILOR XY Raman spectrometer, thus warranting that the same points of the samples were measured in Raman and Luminescence.

## RESULTS AND DISCUSSION

The composition of the layers was estimated from HRXRD and  $\mu$ -R data. The perpendicular lattice mismatches,  $(\Delta d/d)^\perp$ , estimated for the six samples studied were positive, which corresponds to compressive mismatch and therefore to slightly Ga rich stoichiometry, the composition was close to the lattice matched value since the maximum value of  $(\Delta d/d)^\perp$  was  $5.10^{-3}$ .

$\mu$ -R spectra were obtained on different points of the samples. The  $\mu$ -PL spectra were obtained on the same points, which allowed a correlation between both measurements. The Raman spectrum of InGaP presents a two mode behaviour [7]. It consists of an LO phonon mode (GaP like) at  $380\text{ cm}^{-1}$  (henceforth labeled  $\text{LO}_1$ ), a TO phonon mode (InP-like,  $\text{TO}_2$ ) at  $330\text{ cm}^{-1}$ , which is selection rule forbidden, but is activated by alloy disorder, figure 2. Special mention should be paid to the phonon band at  $365\text{ cm}^{-1}$ , which has been associated with the InP-like LO phonon ( $\text{LO}_2$ ), the properties of this band have been reported to be sensitive to the spontaneous order. This band seems to have a complex character, in fact a TO band, GaP-like ( $\text{TO}_1$ ) seems to be located in the same spectral region [8]. On the other hand, the frequencies and relative intensities of the modes are dependent on the composition.

There is a clear difference between the Raman spectra of doped and undoped layers. The phonon bands are broadened and the forbidden TO band is enhanced in the doped layers. This is the consequence of the existence of LOPC modes [8]. Therefore, a comparison between the Raman spectra of doped and undoped layers must be done with caution.

The  $\text{LO}_1$  phonon can be used to determine the composition of the layers since its Raman shift is weakly affected by the spontaneous order [7]. The  $\text{LO}_1$  phonon frequency shifts almost linearly with  $x$ ; it increases by  $0.7\text{ cm}^{-1}/\%\text{Ga}$ , in the lattice matched composition range [9]. According to the X-Ray data the samples were slightly Ga-rich. This is confirmed by Raman spectroscopy, since the Raman frequencies were all above the Raman frequency for lattice matching, which is  $382\text{ cm}^{-1}$ ; therefore the layers were slightly Ga-rich ( $\sim 52\%$  Ga). The average Raman shifts measured are  $382.83\text{ cm}^{-1}$  (sample B),  $382.85\text{ cm}^{-1}$  (sample D),  $382.52\text{ cm}^{-1}$  (sample F),  $382.37\text{ cm}^{-1}$  (sample H),  $382.50\text{ cm}^{-1}$  (sample I) and  $385.89\text{ cm}^{-1}$  (sample J). Samples B, D, F, H and I have compositions that differ each other by less than 1%. Sample J presents a large Raman shift that can be interpreted as a Ga rich composition ( $\approx 55\%$ ).

The Raman scattering is sensitive to the atomic arrangement; in fact, spontaneous CuPt-type order was observed to influence the Raman spectrum. An empirical relation between the band gap and the depth of the valley between the two LO peaks in the Raman spectrum was reported [10]. The valley depth normalized to the intensity of the  $\text{LO}_2$  phonon peak is taken as an order parameter, labeled S, see figure 2. The existence of a profound valley between the two LO bands (high S) corresponds to a large band gap (disordered layer), a value of 0.6 has been reported for fully disordered specimens. The valley depth decreases for partially ordered samples, reaching a value of 0.2 for fully ordered samples [7,10].

The Raman spectra were obtained at several points of the layers using the Raman microprobe. The Raman parameters of the spectra, that is, Raman Shifts  $\omega_{\text{LO}_1}$  and  $\omega_{\text{LO}_2}$  and the FWHM (Full Width at Half Maximum) of the modes were studied in relation to the valley depth aiming to establish a correlation between spontaneous order and the Raman parameters. The FWHM of the peaks is related to the phonon correlation length. In fact, the FWHM should decrease when In and Ga are randomly distributed in the cation sublattice and will increase for

clustering or in the presence of the ordered phase. The FWHM of the LO<sub>1</sub> band was observed to increase with the valley depth, which is controversial with the above interpretation. A good correlation is found for the frequency splitting between both LO modes,  $\Delta\omega_{LO} = (\omega_{LO1} - \omega_{LO2})$ , and the valley depth, figure 3. The valley depth increases when this splitting increases. This cannot be related to composition changes since the major contribution to this splitting is due to the down frequency shift of the LO<sub>2</sub> Raman band, the LO<sub>1</sub> band frequency remaining within the limits determined by the small composition variation above discussed, figure 3. According to the above discussion, a shift to the low frequency of  $\omega_{LO2}$  takes place with a broadening of the LO<sub>1</sub> band. These data are only referred to the undoped samples, since the spectra obtained for doped samples, I and J, are influenced by the LOPC modes.

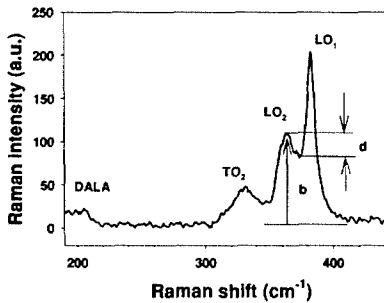


**Figure 2..** Typical Raman spectra of lattice matched InGaP/GaAs. The order parameter, S, is defined as the valley depth, d, normalized to the intensity of the LO<sub>2</sub> band, b ( $S=d/b$ )

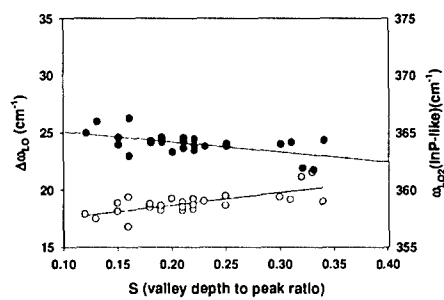


**Figure 3..**  $\Delta\omega_{LO}(\omega_{LO1}-\omega_{LO2})$  (●) and  $\omega_{LO2}$  (InP-like) (○) vs S

Taking the band gap as the peak energy of the intrinsic PL band at room temperature one obtains the following band gap average energies for the samples: 1.90 eV (sample B), 1.87 eV (sample D), 1.85 eV (sample F), 1.86 eV (sample H), 1.91 eV (sample I) and 1.89 eV (sample J). The PL spectra were measured at the same points that the Raman spectra.

The band gap is also influenced by the layer composition. In the lattice matched region the band gap is enlarged by 15 meV for an increase of 0.01 in the molar fraction of Ga [11]. However, the composition of samples B, D, F, H and I was observed to lay within less than 1% percent interval. Therefore, one can assume that the band gap differences between these samples are mostly due to the degree of spontaneous order. Only the band gap measured for sample J could be additionally contributed by composition deviation from the lattice matched value, according to the Raman data. The largest band gap and therefore the lowest degree of spontaneous order corresponds to samples B and I, followed by sample D and finally the higher degree of order corresponds to samples F and H. Taking into account the characteristics of the samples one can argue that: i) n-type substrates benefit the spontaneous order, the degree of order increases with the dopant concentration of the substrate, ii) SI substrates reduce the degree of spontaneous order, iii) Zn doping randomizes the alloy, which is a well known property of Zn [12].

If one plots the band gap vs the order parameter, S, for the undoped samples one observes that the expected correlation does not appear, figure 4. The samples with the largest band gap, B

and D, have small S, while the samples with the smallest band gap have higher values of S. This result is controversial with the results reported by other authors. This can be explained on the basis of the complex nature of the Raman band labeled LO<sub>2</sub> and the surface topography of our samples. The samples grown on SI substrates present a rough topography with high index planes, while the topography of the samples grown on n-type substrates was smooth, see figure 1. In our scattering geometry the TO bands are forbidden, however, they can be activated by either alloy fluctuation or the surface orientation. The presence of high index planes in samples B and D should activate the forbidden TO<sub>1</sub> mode, with the corresponding lineshape change of the band at 365 cm<sup>-1</sup>, up to now called LO<sub>2</sub>, which would result on a reduction of S in spite of the lower spontaneous CuPt-type order of these samples. The smooth surface of samples F and H should reduce the contribution of the forbidden TO<sub>1</sub> mode to the LO<sub>2</sub> Raman band. An attentive observation of the spectra of samples B and D shows that the decrease of S is accompanied by an increase of the intensity of the other TO phonon band (InP-like, TO<sub>2</sub>) at 330 cm<sup>-1</sup>, figure 5, which is consistent with the activation of the TO forbidden modes and the contribution of the TO<sub>1</sub> mode to the value of S.

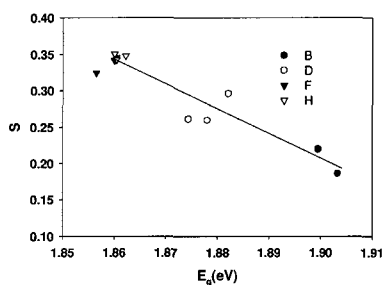


**Figure 4.** S vs E<sub>g</sub>(nm). The line is a guide to the eye

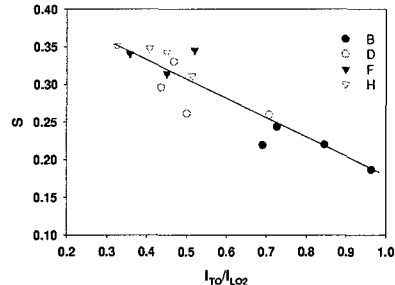


**Figure 5.** S vs I<sub>TO2</sub> / I<sub>LO2</sub>, TO<sub>2</sub> is the band at 330 cm<sup>-1</sup>. The straight line is a guide to the eye.

Finally, monochromatic (intrinsic emission) intensity PL maps were obtained for the different samples at room temperature. Intensity fluctuations were observed, figure 6. The intrinsic PL intensity is governed by the competition between band to band recombination and non radiative recombination at deep levels. Also a decrease of the luminescence intensity has been reported (up to a factor 3) for the ordered phase [11]. Raman data did not reveal significant composition changes over a sample. However, a correlation between the PL intensity and the peak energy was observed in samples grown on n-type substrates, see Fig. 6. Therefore, the non-uniformities of the PL intensity and peak wavelength can be understood if one considers that the PL intensity and band gap energy changes are controlled by the ordered/disordered volume ratio probed by the laser beam.

The influence of the substrate on the characteristics of the samples can be tentatively explained by the change in the lattice parameter introduced by the Si impurities, since the other growth parameters were the same for all the growth runs. The smooth layer by layer growth allows the segregation of cations, while the tridimensional growth avoids it.

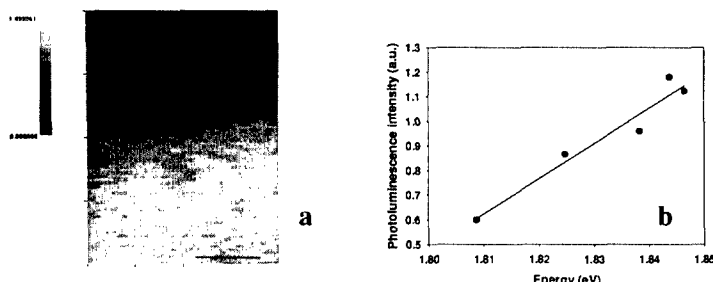


**Figure 6.** Monochromatic PL map (room temperature) of sample F, (a). The bar is 1 mm.  $I_{PL}$  vs Eg measured in sample F (b).

## CONCLUSIONS

The influence of the type of substrate on the order of lattice matched InGaP/GaAs layers was studied by  $\mu$ -R and  $\mu$ -PL. The Si doping of the substrates benefits the ordering, which is related to the shrink of the band gap. The Raman parameters were demonstrated to be also influenced by the surface topography, since the S parameter was related to the activation of the forbidden  $TO_1$  (GaP-like) Raman mode, therefore, S cannot be used as a measure of the order for samples with rough surface. Spatial inhomogeneities were related to the distribution of the ordered / disordered domains.

**ACKNOWLEDGEMENTS.** The Spanish group was funded by JCL (Junta de Castilla y León) and FES (Fondo Social Europeo) (Project: VA047/01). The Italian group acknowledges the financial support of the Italian Space Agency.

## REFERENCES

1. J.R. Shealy, C.F. Schaus, L.F. Eastman; *Appl. Phys. Lett.* **48**, 242 (1986)
2. T.F. Kuech, D.J. Wolford, E. Venhoff, V. Deline, P.M. Mooney, R. Potemski, J. Bradley; *J.Appl. Phys.* **62**, 632 (1987)
3. Y.Q. Wang, Z.L. Wang, T. Brown, A. Brown, G. May; *J. Electron. Mater.* **29**, 1372 (2000)
4. Krost, N. Esser, H. Selber, J. Christen, W. Richter, D. Bimberg, L.C. Su, G.B. Stringfellow; *J. Vac. Sci. Technol.* **12**, 2558 (1994)
5. S.F.Yoon, K.W.Mah, H.Q.Zheng; *Opt. Mater.* **14**, 59 (2000)
6. Sasaki, K. Tsuchida, Y. Narukawa, Y. Kawakami, S.G. Fujita, Y. Hsu, G.B. Stringfellow; *J.Appl. Phys.* **89**, 343 (2001)
7. F.Alsina, N.Mestres, J.Pascual, C.Geng, P.Ernst, F.Scholz; *Phys.Rev. B* **53**, 12994 (1996)
8. K.Sinha, A. Mascarenhas, S.R.Kurtz, J.M.Olson; *J.Appl.Phys.* **78**, 2515 (1995)
9. M. Zachau, W.T. Masselink; *Appl. Phys. Lett.* **60**, 2098 (1992)
10. T. Suzuki, A. Gomyo, S. Iijima, K. Kobayashi, S. Kawata, T. Hino, T. Yuasa; *Jpn. J. Appl. Phys.* **27**, 2098 (1988)
11. G.H. Olsen, C.J. Nuese, R.T. Smith; *J. Appl. Phys.* **49**, 5523 (1978)
12. T. Suzuki, A.Gomyo, K.Kobayashi, S. Kawata, S.Iijima; *Jpn. J. Appl. Phys.* **27**, L1549 (1988)